Numerical study of a dual representation of the integer quantum Hall transition

Kevin S. Huang[1], S. Raghu[1,2], Prashant Kumar[1,3]
[1]*Stanford Institute for Theoretical Physics, Stanford University, Stanford, California 94305, USA*
[2]*Stanford Institute for Materials and Energy Sciences, SLAC National Accelerator Laboratory, Menlo Park, CA 94025, USA*
[3]*Department of Physics, Princeton University, Princeton, New Jersey 08544, USA*
(Dated: September 18, 2020)

We study the critical properties of the non-interacting integer quantum Hall to insulator transition (IQHIT) in a 'dual' composite-fermion (CF) representation. A key advantage of the CF representation over electron coordinates is that at criticality, *CF states are delocalized at all* energies. The CF approach thus enables us to study the transition from a new vantage point. Using a lattice representation of CF mean-field theory, we compute the critical and multifractal exponents of the IQHIT. We obtain $\nu = 2.56 \pm 0.02$ and $\eta = 0.51 \pm 0.01$, both of which are consistent with the predictions of the Chalker-Coddington network model formulated in the electron representation.

Introduction - The integer quantum Hall (QH) to insulator transition (IQHIT) is one of the best studied topological phase transitions in condensed matter physics[1–6]. Without interactions, the existence of a quantum Hall plateau requires quenched disorder, and a magnetic field tunes the system from a quantum Hall (QH) state to an Anderson insulator. A beautiful representation of the IQHIT known as the Chalker-Coddington model (CCM) involves percolation of droplets of IQH and insulating phases[7]. The CCM has been amenable to large scale numerical studies of critical exponents of the non-interacting IQHIT[8].

Nevertheless, all electron representations of the IQHIT suffer with a key drawback: it has been difficult to include electron-electron interaction effects, which are necessary to account for very basic aspects of the IQHIT. For instance, interactions are necessary to ensure a non-zero finite temperature electrical resistivity[9]. Other aspects of the transition - dynamical scaling laws and the issue of whether or not integer and abelian fractional QH transitions are governed by the same universality class - requires the inclusion of interactions. Thus, there is a need for alternate formulations of the QHIT, which can more easily address such questions.

In this letter we present a first step in devising alternate formulations of the QHIT, making use of a dual composite fermion (CF) representation. The idea that CFs are dual 'vortices' of electrons has been made precise in a remarkable set of recent developments[10,11]. As we show below, in a mean-field approximation, the CF formulation of the IQHIT belongs to the same universality class as the one studied in electron coordinates. However, it offers several distinct advantages[12]: most interestingly, delocalized states occur over all energies[13,14] at the IQHIT in the CF representation enabling a finite dc conductivity as $T \to 0$. Furthermore, a CF theory can more readily incorporate interaction effects, and can treat integer and fractional QHITs on equal footing[15].

The phase diagram of the IQHIT is realized in the CF representation as follows: first, the integer QH state of electrons with $\sigma_{xy} = e^2/h$ maps onto an integer QH state of CFs but with opposite Hall conductivity. Second, the electron insulator is a CF insulator. It only remains to show that the critical exponents obtained in the CF representation are identical to those predicted by the CCM.

Using a tight-binding regularization of a CF hamiltonian, we compute two critical exponents, ν and η describing respectively the divergence of the localization length, and the multifractal scaling exponents at criticality. Specifically, we find $\nu = 2.56 \pm 0.02$, and $\eta = 0.51 \pm 0.01$, both of which are in excellent agreement with established results obtained from the CCM.[16–26] Thus, we establish that the IQHIT as viewed in CF coordinates is governed by the same fixed point as the CCM. This observation opens new possibilities in studies of the IQHIT, where interaction effects may be included more readily.

IQHIT in the idealized CF model - 2D electrons in a perpendicular magnetic field B can be transformed, via an exact mapping ("flux attachment")[27] to CFs that couple to the sum of the external and "statistical" flux $B + b(r)$.[28,29] When two quanta of flux are attached to each electron, there is an exact identity relating the CF density to the statistical flux: $b(r) = -4\pi n(r)$. CF mean-field theory results from "smearing the flux" and the identity is satisfied only on average: $\langle b(r)\rangle = -4\pi\langle n(r)\rangle$. With a quenched random potential $V(r)$ that varies on length scales large compared to the magnetic length, the linear response is a random density $\delta n(r) = \chi V(r)$, where $\chi = m/2\pi$ is the uniform compressibility[30]. Thus, in CF mean-field theory, there is a slaving[13,31] between $V(r)$ and $b(r)$:[32] $V(r) = -b(r)/2m$. Furthermore, for asymptotic behavior near criticality, we can ignore non-linear response effects, and study the following model Hamiltonian density:

$$h(r) = c^\dagger \left[\frac{(-i\boldsymbol{\partial} - \boldsymbol{a})^2}{2m} + \frac{g}{2}\frac{b(r)}{2m} - \mu \right] c, \quad b(r) = \epsilon_{ij}\partial_i a_j. \tag{1}$$

It involves free, spin-polarized fermions with parabolic dispersion coupled to a random vector potential $\boldsymbol{a}(r)$, along with a "gyromagnetic term" $\frac{g}{2}b(r)/2m$. In the above context of CF mean-field theory with long-wavelength disorder, $g = 2$.

Surprisingly, when $g = 2$, the system undergoes an IQHIT as the spatial-average magnetic field $b_0 \equiv \bar{b}(r)$ changes sign. To see why, observe that when $b_0 \neq 0$, all finite energy states are localized in the thermodynamic limit at $T = 0$. However, there are exact *zero energy modes*[33] for $b_0 < 0$, which behave as a filled Landau level. The zero modes are absent for $b_0 > 0$. As a consequence, the zero temperature phases are IQH (insulating) states for $b_0 < 0 (b_0 > 0)$. At the critical point ($b_0 = 0$), the Hall conductivity can be computed *analytically* for the Hamiltonian above, and is $\sigma_{xy} = -e^2/2h$.[34] It follows from the contrapositive of Laughlin's gauge argument that states at all energies are *delocalized* when $b_0 = 0$. Our present goal is to obtain critical exponents associated with this transition using a lattice realization of the above problem.

Lattice model - The lattice analog of the above consists

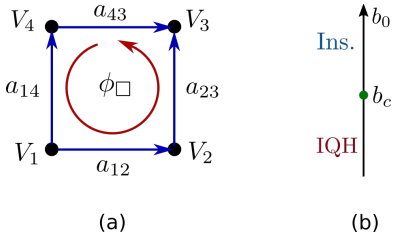

FIG. 1. (a) The tight-binding model on a square lattice for the Hamiltonian of Eq. 2. There is a quenched chemical potential on its sites while quenched vector potential on the links. The flux through the square plaquette is proportional to the average potential on the four attached vertices as per Eq. 4. (b) The phase diagram of the lattice model. In the idealized limit, $b_0 < 0$ and $b_0 > 0$ correspond to the $\nu_{\rm cf} = -1$ IQH state and the Anderson insulator respectively. A topological phase transition between the two occurs at $b_0 = b_c = 0$.

of CFs on a square lattice with nearest neighbor hopping (we set the lattice spacing to unity). Quenched random scalar and vector potentials live on the lattice sites and links respectively (Fig. 1):

$$\mathcal{H}_{\rm lattice} = -\sum_{\langle ij \rangle} c_i^\dagger \left[t e^{i a_{ij}} + \mu \delta_{ij} \right] c_j - \sum_i V_i c_i^\dagger c_i, \quad (2)$$

where i, j label lattice sites, and $a_{ij} = -a_{ji}$ are associated with the directed nearest-neighbor link connecting sites i and j. Random fluxes are associated with each square plaquette of the lattice.

We slave the random chemical potential to the random flux as follows. Consider a square plaquette, whose vertices are lattice sites labeled $1 - 4$ in a counterclockwise sense (Fig. 1). We equate the flux asscociated with the plaquette,

$$\phi_\square = a_{12} + a_{23} + a_{34} + a_{41}, \quad (3)$$

with the *average* of the 4 random potentials V_i:

$$\phi_\square = b_\square = -\frac{m}{g} \sum_{i=1}^{4} V_i, \quad (4)$$

where, for simplicity, we take the mass to be the effective mass of the clean tight-binding model at the bottom of the band, i.e. $m = 1/2t$. We repeat the procedure for all elementary plaquettes of the lattice. We choose $V_i, i \in 1 \cdots 4$ from an independent uniform distribution $V_i \in [-W/2 + V_0, W/2 + V_0]$, where $V_0 = -g b_0/m$ and W measures the strength of the disorder.

Therefore, for a weak, long range disorder and Fermi energy close to the bottom of the band, the Hamiltonian in Eq. 2 can be approximated as:

$$\mathcal{H}_{\rm lattice} \approx \frac{(\boldsymbol{p} - \boldsymbol{a})^2}{2m} + \frac{g}{2} \frac{b(\boldsymbol{r})}{2m} - 4t. \quad (5)$$

Notice that since the flux through each plaquette is bounded in magnitude by π, we have $|W/2 \pm V_0| \leq g\pi/4m$. In principle one could adopt a more sophisticated procedure whereby the compressibiilty is determined in a self-consistent manner in equating the potential and flux disorders. We choose not to do so for simplicity: as we show below the simple procedure employed here is already sufficient to capture the universal properties associated with the critical point, provided the Fermi energy remains sufficiently close to the band-bottom to warrant an effective mass approximation.

Figure 2 displays the density of states over the entire bandwidth of the lattice model above, for non-zero b_0. The lattice model increasingly accurately captures the behavior of the ideal model above in the limit where the Fermi level is close to the band bottom and the disorder is weak. For practical numerical calculations, however, it will be useful to use strong disorder which allows for shorter localization lengths and hence for better finite-size scaling behavior near the critical point. This deviation from weak and long-wavelength disorder, as well as lattice corrections to the effective mass approximation, lead to a shift in the location of the phase transition as a function of b_0: in general, the IQHIT occurs at a finite value of b_0, which approaches zero as the idealized limit of the previous section is approached.

Localization length exponent - Employing the standard transfer matrix techniques,[35,36] we study the behavior of the localization length in the CF model above. We realize the tight-binding model on a quasi-1D cylinder of dimensions $L \times M$, where L is the length of the cylinder along its axis while M is the circumference. We obtain the localization length $\xi_M(b_0)$ along the axis of the cylinder as a function of b_0 and the system width M with $g = 2$. In the 2D limit, i.e. $M \to \infty$, it diverges as $\xi_\infty(b_0) \sim |b_0 - b_c|^{-\nu}$ near the critical point with the critical exponent ν. We obtain ν via the finite-size scaling of the dimensionless localization length: $\Lambda_M(b_0) \equiv \xi_M(b_0)/M$ near the critical point.[37] To achieve this, we fit our data to the following polynomial function:

$$\Lambda_M(b_0) = \sum_{n=0}^{N_R} a_n \left(M^{1/\nu} \Delta \right)^n + \psi M^{-y} + c_{11} \psi \Delta M^{1/\nu} M^{-y} \quad (6)$$

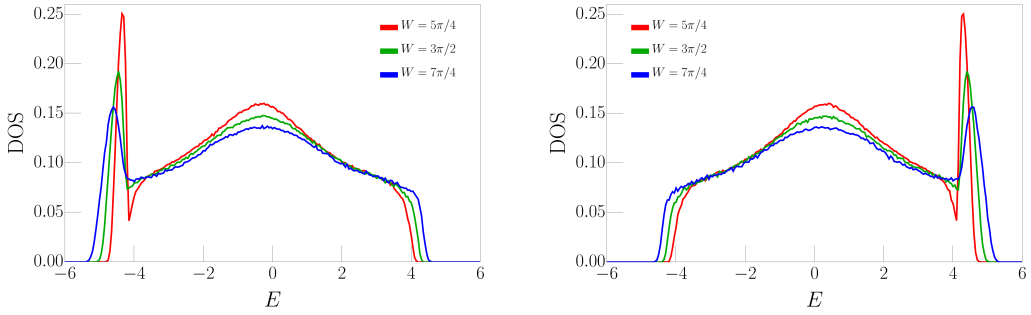

FIG. 2. The density of states of the lattice Hamiltonian (2) for various disorder strengths and (a) $b_0 = -0.5$ (b) $b_0 = 0.5$. There are zero-modes near the bottom of the band for $b_0 < 0$ which become sharper as the disorder strength is reduced. Further, the zero modes levitate up for $b_0 > 0$. Thus, the lattice model faithfully describes the idealized Hamiltonian of Eq. 1 in the weak disorder limit and when the Fermi energy is near the bottom of the band.

where N_R is the degree of the polynomial in the relevant parameter $\Delta \equiv b_0 - b_c$. ψ is the amplitude of the leading irrelevant operator and y is the corresponding correction to scaling exponent. Further, a_n, c_{11} and b_c are fitting parameters, the last of which gives the location of the transition.

For $W = 3\pi/2$ and Fermi energy $E_F = -4$ at $g = 2$, we plot the calculated $\Lambda_M(b_0)$ in Fig. 3(a). Fitting the data to the above polynomial form using the standard least square error method, we extract $\nu = 2.56 \pm 0.02$. Also, for a stronger disorder: $W = 7\pi/4$, we find $\nu = 2.57 \pm 0.02$ (Fig. 3(b)) suggesting that the exponent is independent of disorder strength. These results are in agreement with the previous studies of the IQHIT inspired by the electron version of the transition including the Chalker-Coddington model.[7,16–25] They support the idea that the two descriptions of IQHIT lead to the same universal behavior. In addition, we note that our results are slightly inconsistent with studies based on other models reporting a smaller exponent.[38–40]

Multifractal scaling - In addition to the localization length exponent ν, wavefunction multifractality represent additional universal characteristics of the IQHIT. They correspond to the finite size scaling of the inverse participation ratios P_q calculated from the critical wavefunction ψ:

$$P_q \equiv L^d \langle |\psi|^{2q} \rangle \propto L^{-2(q-1)-\Delta(q)}. \tag{7}$$

where L is the system size and $d = 2$. Employing standard techniques,[41,42] we calculate these exponents using the critical wavefunctions of a square system of dimensions $L \times L$ with periodic boundary conditions. Since the total flux through the sample is quantized in the units of 2π, we round b_c obtained in the previous section to the nearest integer multiple of $2\pi/L^2$.

For the critical point in Fig. 3(a) at $b_0 = -0.229$, we find $\eta \equiv -\Delta(2) = 0.51 \pm 0.01$. And for the critical point in Fig. 3(b) at $b_0 = -0.558$, we get $\eta = 0.52 \pm 0.01$. These are close to the value $\eta = 0.5425$ obtained in Ref. 26. Further, they are also consistent with $\eta = 0.5$ predicted in Ref. 43. We plot the full multifractal spectra in Fig. 4 and fit them to the following form symmetric around $q = 1/2$:[26,44]

$$\Delta(q) = 2q(1-q)\left[\gamma_0 + \gamma_1 (q - 1/2)^2 + \gamma_2 (q - 1/2)^2\right]. \tag{8}$$

We find $\gamma_0 = 0.129 \pm 0.005, \gamma_1 = 0.003 \pm 0.003, \gamma_2 = -0.0002 \pm 0.0004$ and $\gamma_0 = 0.133 \pm 0.006, \gamma_1 = 0.002 \pm 0.004, \gamma_2 = -0.00005 \pm 0.00050$ for the two critical points. These are in excellent agreement with the corresponding quantities in Ref. 26. Likewise, we also find evidence for corrections to the proposed parabolic form[45–47] since $\gamma_1 \neq 0$. It should be noted that our data does not show a perfect symmetry around $q = 1/2$. A possible cause for this is that the critical points were located using the transfer matrix method, which are likely slightly different for a square sample of finite size due to the different aspect ratio and boundary conditions. We summarize the results of all obtained critical exponents in Table I.

While the value $g = 2$ in Eq. 1 is motivated by CF mean-field theory, we can consider the effect of relaxing the value of g on the IQHIT. Such deviations from $g = 2$ can arise from lattice corrections to the effective mass approximation, or from the breaking of particle-hole symmetry in the disorder-averaged theory[48]. As we show in Appendix A, the localization length exponent decreases monotonically with g. The extent to which such deviations reflect a new universality class for the IQHITs, or are due to substantial finite size effects, or from large corrections to scaling from irrelevant operators, remain unclear and require further study. We shall return to these questions in future work.

Discussion - Our results have several important implications for the IQHIT, and suggest several new directions of exploration. The most important implication of our study governs finite temperature dc transport in the quantum critical regime. In electron coordinates, extended states occur at a single energy, and without any interaction effects, $\rho_{xx}(T \to 0) \neq \rho_{xx}(T = 0)$. By contrast, in the CF representation, this issue does not arise,

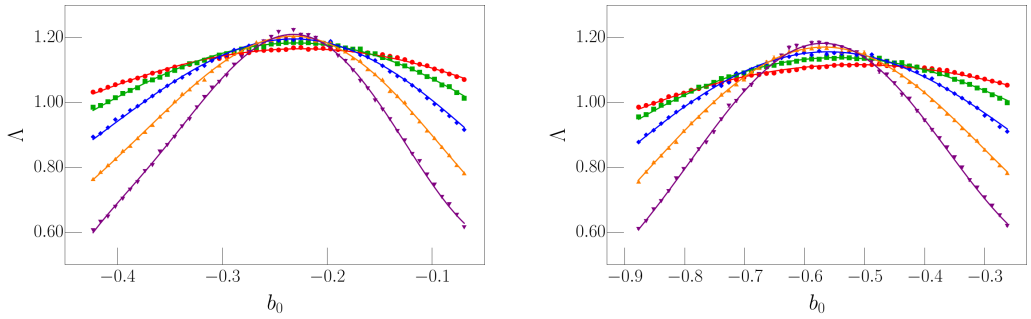

(a) (b)

FIG. 3. The scaling of the renormalized localization length as a function of the cylinder width M and the tuning parameter b_0 at Fermi energy $E_F = -4$ and (a) $W = 3\pi/2$, (b) $W = 7\pi/4$. The red dots, green squares, blue rotated-squares, orange triangles, purple upside-down-triangles correspond to $M = 16, 32, 64, 128, 256$ respectively. We have set $L = 10^7$ for all the data points. The best fit to Eq. (6) is drawn with solid lines and we obtain the critical exponent (a) $x = 2.56 \pm 0.02$, (b) $x = 2.57 \pm 0.02$. The critical points are found to be located at $b_0 = b_c$ where (a) $b_c = -0.229$ and (b) $b_c = -0.558$. Since the critical point moves towards $b_c = 0$ as the disorder is made weaker, the idealized limit of Eq. 1 is approached.

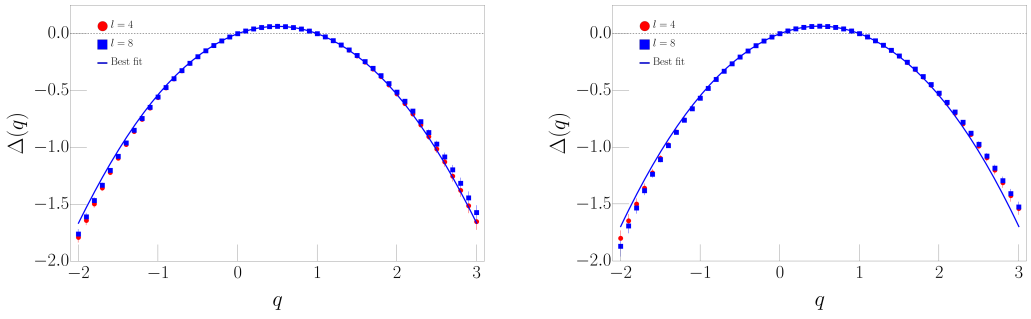

(a) (b)

FIG. 4. The numerically calculated multifractal spectrum $\Delta(q)$ at Fermi energy $E_F = -4$ for disorder strength (a) $W = 3\pi/2$ and (b) $W = 7\pi/4$ at $g = 2$. The critical points are taken to be located at (a) $b_0 = 0.229$ and (b) $b_0 = -0.558$. We average $|\psi|^2$ over a box of dimensions $l \times l$ to rid it of the short distance correlations between wavefunction amplitudes. Further averaging over 1000 wavefunctions reduced fluctuations coming from the randomness of the disorder configurations. The red dots, blue squares correspond to $l = 4, 8$ respectively. Using system sizes $L = 32, 64, 128$ and 256, $\Delta(q)$ is obtained by performing finite size scaling according to Eq. (7). Note that $\Delta(1) = \Delta(0) = 0$ by definition. Further, the best fit to Eq. (8) using $l = 8$ data is drawn with the solid blue line and we get (a) $\gamma = 0.129 \pm 0.005$, (b) $\gamma = 0.133 \pm 0.006$.

Parameters	ν	η	γ_0
$W = 3\pi/2$ $b_0 = -0.229$	2.56 ± 0.02	0.51 ± 0.01	0.129 ± 0.005
$W = 7\pi/4$ $b_0 = -0.558$	2.57 ± 0.02	0.52 ± 0.01	0.133 ± 0.006

TABLE I. A summary of exponents at Fermi energy $E_F = -4$ and $g = 2$.

since extended states occur over a range of energies at criticality. Indeed, a finite CF resistivity implies the same for the electrical resistivity via the exact relation[49]

$$\rho_{\rm cf}^{ab} = \rho_{\rm el}^{ab} + 4\pi\epsilon^{ab}, \quad \epsilon^{ab} = \begin{pmatrix} 0 & 1 \\ -1 & 0 \end{pmatrix}. \tag{9}$$

It is thus the CF representation that guarantees a smooth $T \to 0$ limit of the resistivity tensor in mean-field theory.

Second, the success of the CF mean-field theory suggests new analytic approaches to describing the non-interacting IQHIT. Recent work has shown that the effective theory governing disorder averaged quantities in the weak-coupling regime $\sigma_{xx}^{\rm cf} \gg 1$, is a non-linear sigma model with a topological term, similar to the theory put forward in electron coordinates[15]. However, such theories run to strong coupling, since the critical point itself occurs at $\sigma_{xx}^{\rm cf} \sim \mathcal{O}(1)$. An analytic description of such a transition still remains unknown. It is likely that the CF representation may give way to new analytic treatments. One possible route is to note that the theory

in Eq. 1 is equivalent to a 2-component Dirac fermion at finite chemical potential in the presence of a random vector potential. The non-abelian bosonization of the Dirac fermion may lead to new descriptions in terms of Wess-Zumino-Witten (WZW) models.[45] We shall report progress on such analytic treatments in future studies.

Conclusions - In summary, we have calculated the critical and multifractal exponents for the IQHIT using a composite-fermion representation, which are in good agreement with numerical studies of the Chalker-Coddington network model. While the electron and CF formulations have distinct origins, they are expected to flow to the same IR fixed point governing the IQHIT: in this sense, the electron and CF formulations are thus 'dual' to one another.

Acknowledgement: We thank S. Kivelson and Jun Ho Son for fruitful discussions. K.H. was supported in part by the Department of Physics, Stanford University through an undergraduate summer research fellowship. S.R. and P.K. were supported in part by the US Department of Energy, Office of Basic Energy Sciences, Division of Materials Sciences and Engineering, under contract number DE-AC02-76SF00515. P.K. was supported in part by DOE grant No. DE-SC0002140.

[1] H. P. Wei, D. C. Tsui, M. A. Paalanen, and A. M. M. Pruisken, Phys. Rev. Lett. **61**, 1294 (1988).
[2] L. W. Engel, D. Shahar, i. m. c. Kurdak, and D. C. Tsui, Phys. Rev. Lett. **71**, 2638 (1993).
[3] D. Shahar, D. C. Tsui, M. Shayegan, R. N. Bhatt, and J. E. Cunningham, Phys. Rev. Lett. **74**, 4511 (1995).
[4] D. Shahar, D. C. Tsui, M. Shayegan, E. Shimshoni, and S. L. Sondhi, Science **274**, 589 (1996).
[5] K. Yang, D. Shahar, R. N. Bhatt, D. C. Tsui, and M. Shayegan, Journal of Physics: Condensed Matter **12**, 5343 (2000).
[6] S. L. Sondhi, S. M. Girvin, J. P. Carini, and D. Shahar, Rev. Mod. Phys. **69**, 315 (1997).
[7] J. T. Chalker and P. D. Coddington, J. Phys. C: Solid State Phys. **21**, 2665 (1988).
[8] B. Huckestein and M. Backhaus, Phys. Rev. Lett. **82**, 5100 (1999).
[9] Z. Wang, M. P. A. Fisher, S. M. Girvin, and J. T. Chalker, Phys. Rev. B **61**, 8326 (2000).
[10] D. T. Son, Phys. Rev. X **5**, 031027 (2015).
[11] N. Seiberg, T. Senthil, C. Wang, and E. Witten, Annals of Physics **374**, 395 (2016), arXiv:1606.01989 [hep-th].
[12] While the non-interacting electron theory of the IQHIT is justified for short range density-density interactions, which are irrelevant in the RG sense at the IQHIT[50], CF mean-field theory is applicable when these interactions are long ranged.
[13] P. Kumar, M. Mulligan, and S. Raghu, Phys. Rev. B **98**, 115105 (2018).
[14] P. Kumar, Y. B. Kim, and S. Raghu, Phys. Rev. B **100**, 235124 (2019).
[15] P. Kumar, P. A. Nosov, and S. Raghu, (2020), arXiv:2006.11862 [cond-mat.str-el].
[16] D.-H. Lee, Z. Wang, and S. Kivelson, Phys. Rev. Lett. **70**, 4130 (1993).
[17] K. Slevin and T. Ohtsuki, Phys. Rev. B **80**, 041304 (2009).
[18] H. Obuse, A. R. Subramaniam, A. Furusaki, I. A. Gruzberg, and A. W. W. Ludwig, Phys. Rev. B **82**, 035309 (2010).
[19] M. Amado, A. V. Malyshev, A. Sedrakyan, and F. Domínguez-Adame, Phys. Rev. Lett. **107**, 066402 (2011).
[20] I. C. Fulga, F. Hassler, A. R. Akhmerov, and C. W. J. Beenakker, Phys. Rev. B **84**, 245447 (2011).
[21] K. SLEVIN and T. OHTSUKI, International Journal of Modern Physics: Conference Series **11**, 60 (2012), https://doi.org/10.1142/S2010194512006162.
[22] H. Obuse, I. A. Gruzberg, and F. Evers, Phys. Rev. Lett. **109**, 206804 (2012).
[23] W. Nuding, A. Klümper, and A. Sedrakyan, Phys. Rev. B **91**, 115107 (2015).
[24] M. Puschmann, P. Cain, M. Schreiber, and T. Vojta, Phys. Rev. B **99**, 121301 (2019).
[25] B. Sbierski, E. J. Dresselhaus, J. E. Moore, and I. A. Gruzberg, (2020), arXiv:2008.09025 [cond-mat.mes-hall].
[26] F. Evers, A. Mildenberger, and A. D. Mirlin, Phys. Rev. Lett. **101**, 116803 (2008).
[27] S. C. Zhang, T. H. Hansson, and S. Kivelson, Phys. Rev. Lett. **62**, 82 (1989).
[28] V. Kalmeyer and S.-C. Zhang, Phys. Rev. B **46**, 9889 (1992).
[29] B. I. Halperin, P. A. Lee, and N. Read, Phys. Rev. B **47**, 7312 (1993).
[30] The mass m that enters the compressibility is the same as the band mass, which is renormalized by Coulomb interactions. However, no further renormalization occurs due to gauge fluctuations, as shown in Ref. 51.
[31] C. Wang, N. R. Cooper, B. I. Halperin, and A. Stern, Phys. Rev. X **7**, 031029 (2017).
[32] From here on, we change our notation so that $b(r)$ and $a(r)$ represent the "effective" magnetic and gauge fields experienced by the composite fermions. The effective field is related by a shift to the "statistical" gauge field, i.e. $a_{\text{eff.}}(r) = a_{\text{stat.}}(r) - A(r)$.
[33] Y. Aharonov and A. Casher, Phys. Rev. A **19**, 2461 (1979).
[34] We assume that all odd moments of $V(r)$ vanish.
[35] A. MacKinnon and B. Kramer, Phys. Rev. Lett. **47**, 1546 (1981).
[36] A. MacKinnon and B. Kramer, Zeitschrift fr Physik B Condensed Matter **53**, 1 (1983).
[37] K. Slevin and T. Ohtsuki, Phys. Rev. Lett. **82**, 382 (1999).
[38] I. A. Gruzberg, A. Klümper, W. Nuding, and A. Sedrakyan, Phys. Rev. B **95**, 125414 (2017).
[39] M. Ippoliti, S. D. Geraedts, and R. N. Bhatt, Phys. Rev. B **97**, 014205 (2018).
[40] Q. Zhu, P. Wu, R. N. Bhatt, and X. Wan, Phys. Rev. B **99**, 024205 (2019).
[41] B. Huckestein, Rev. Mod. Phys. **67**, 357 (1995).
[42] F. Evers and A. D. Mirlin, Rev. Mod. Phys. **80**, 1355 (2008).
[43] M. R. Zirnbauer, Nuclear Physics B **941**, 458 (2019).
[44] A. D. Mirlin, Y. V. Fyodorov, A. Mildenberger, and F. Ev-

ers, Phys. Rev. Lett. **97**, 046803 (2006).
[45] M. R. Zirnbauer, (1999), arXiv:hep-th/9905054.
[46] M. J. Bhaseen, I. I. Kogan, O. A. Soloviev, N. Taniguchi, and A. M. Tsvelik, Nuclear Physics B **580**, 688 (2000).
[47] A. M. Tsvelik, Phys. Rev. B **75**, 184201 (2007).
[48] For PH-symmetry at $\nu = 1/2$, the Hall conductivity of CFs at $b_0 = 0$ must be $\sigma_{xy}^{\rm cf} = -e^2/2h$. This was shown to be the case for $g = 2$ in Eq. 1 in Ref. 13. However, if $g \neq 2$, the PH-symmetry can be broken.
[49] S. Kivelson, D.-H. Lee, and S.-C. Zhang, Phys. Rev. B **46**, 2223 (1992).
[50] D.-H. Lee and Z. Wang, Phys. Rev. Lett. **76**, 4014 (1996).
[51] Y. B. Kim, A. Furusaki, X.-G. Wen, and P. A. Lee, Phys. Rev. B **50**, 17917 (1994).
[52] A. Pruisken, Nuclear Physics B **235**, 277 (1984).
[53] D. E. Khmelnitskii, ZhETF Pisma Redaktsiiu **38**, 454 (1983).
[54] A. M. M. Pruisken, Phys. Rev. B **32**, 2636 (1985).

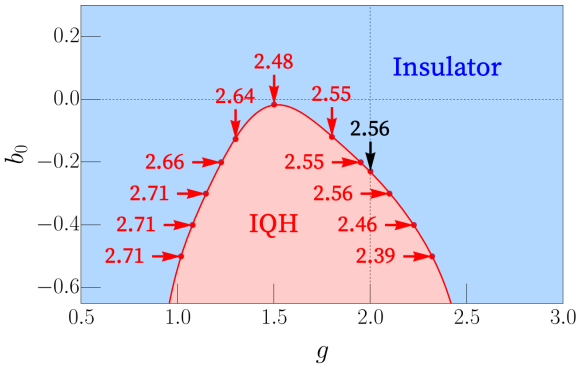

FIG. 5. The phase diagram and critical exponents ν of Hamiltonian in Eq. 2 in the two parameter space of the average magnetic field b_0 and the gyromagnetic ratio g. The parameters are $E_F = -4$, $W = 3\pi g/4$. The IQH state with $\nu_{\rm cf} = -1$ is separated from the insulator through the critical curve drawn in red. The arrows show the critical exponents calculated at various points on this curve. The results suggest that ν decreases as g increases and thus the IQHITs are not in the same universality class. However, a detailed study involving bigger system sizes is needed to show that finite size-effects are not responsible for such a behavior.

Appendix A: Critical scaling in a generalized model

In the main text, we looked at the IQHIT induced by tuning b_0 at $g = 2$ in the CF lattice model of Eq. 2. This was motivated by the fact that b_0 is a physical tuning parameter corresponding to the deviation of electron filling fraction away from $\nu = 1/2$. As mentioned in the main text, deviation away from $g = 2$ can characterize effects such as broken particle-hole symmetry or corrections to the effective mass approximation. Motivated by this, we have studied the phase diagram of the lattice model in the two parameter space of b_0 and g using the transfer-matrix approach.

In the two-parameter space of g and b_0, the IQH phase is separated from the insulating phase by a critical curve. We first obtain the approximate critical curve by calculating Λ_M as a function of g for various slices of the two-parameter space with constant b_0. The critical curve intersects a constant b_0 line at zero-dimensional critical points. These critical points can be located using the fact that at these points Λ_M becomes either a constant or a slightly increasing function of M. Then, by performing a detailed finite-size scaling analysis using Eq. 6 in the vicinity of these points, we obtain both the critical exponent and the precise shape of the critical curve. The results are plotted in Fig. 5. In addition, we provide the data and best fits in Fig. 6.

As can be seen in Fig. 5, the critical exponent ν monotonically decreases as g is increased. Therefore, all the IQHITs may not be in the same universality class and thus the critical exponent may change if PH-symmetry in the electron problem is broken. This is surprising because IQHITs are thought be described by Pruisken's nonlinear sigma model[52] and the two-parameter scaling[53,54] proposed in this context suggests that all critical properties must be identical. However, we think that due to the varying degrees of disorder strengths and finite-size corrections, more rigorous studies involving bigger system sizes and also different techniques are required to resolve the discrepancy between theory and numerics.

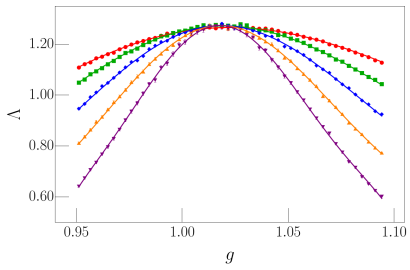

(a) $b_0 = -0.5,\ g = 1.017,\ \nu = 2.71$

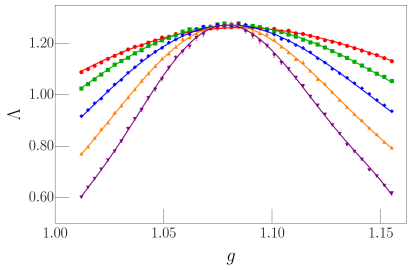

(b) $b_0 = -0.4,\ g = 1.077,\ \nu = 2.71$

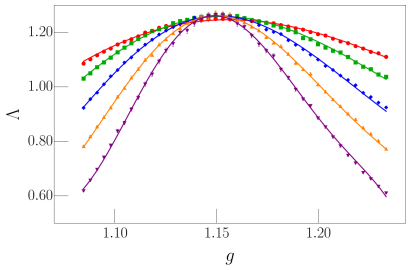

(c) $b_0 = -0.3,\ g = 1.146,\ \nu = 2.71$

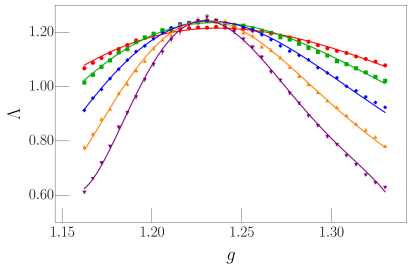

(d) $b_0 = -0.2,\ g = 1.225,\ \nu = 2.66$

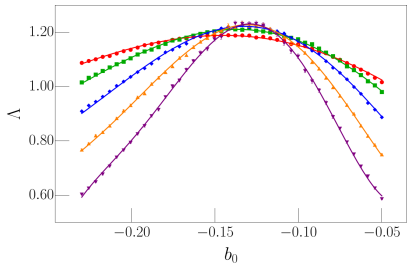

(e) $b_0 = -0.126,\ g = 1.3,\ \nu = 2.64$

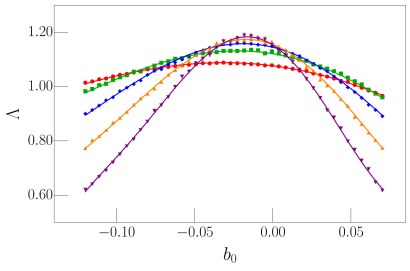

(f) $b_0 = -0.016,\ g = 1.5,\ \nu = 2.48$

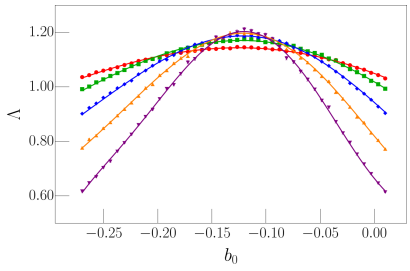

(g) $b_0 = -0.119,\ g = 1.8,\ \nu = 2.55$

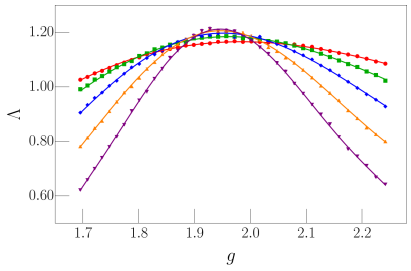

(h) $b_0 = -0.2,\ g = 1.948,\ \nu = 2.55$

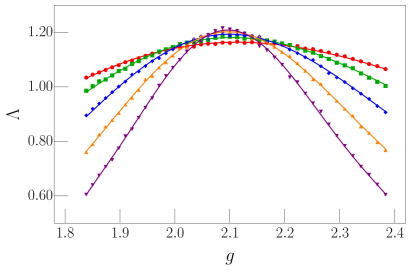

(i) $b_0 = -0.3,\ g = 2.098,\ \nu = 2.56$

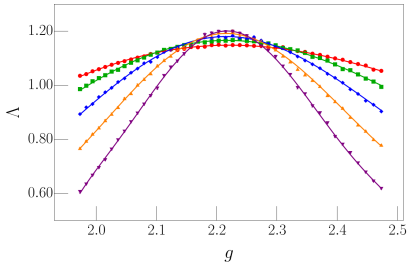

(j) $b_0 = -0.4,\ g = 2.226,\ \nu = 2.46$

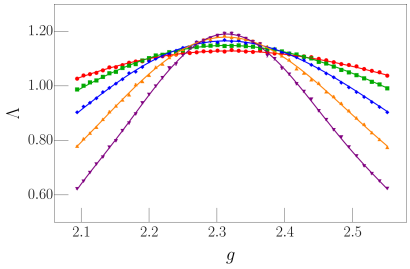

(k) $b_0 = -0.5,\ g = 2.319,\ \nu = 2.39$

FIG. 6. Localization length vs. tuning parameter for the critical points shown in Fig. 5. The tuning parameter is taken to be g for the subfigures (a)-(d) and (h)-(k), while it is b_0 for others. The red dots, green squares, blue rotated-squares, orange triangles, purple upside-down-triangles correspond to $M = 16, 32, 64, 128, 256$ respectively. We have set $L = 10^7$ for all the data points. Further, $W = 3\pi g/4$ and $E_F = -4$. The data around each critical point is fitted to Eq. (6) to obtain the location of the transition and the critical exponent ν. The errors in the critical exponents are approximately 0.02.